Near-infrared laser spectroscopy of NiI

W. S. Tam,[a] Jianjun Ye, and A. S.-C. Cheung[b]
Department of Chemistry, The University of Hong Kong, Pokfulam Road, Hong Kong

(Received 29 June 2004; accepted 23 August 2004)

Laser-induced fluorescence spectrum of NiI in the near infrared region of 714–770 nm has been recorded. Seven bands belonging to three electronic transition systems were observed and analyzed: the (0,0), (1,0), and (2,0) bands of $[13.3]\,^2\Sigma^+$-$A\,^2\Pi_{3/2}$ system; the (1,1) and (0,1) bands of $[13.9]\,^2\Pi_{3/2}$-$X\,^2\Delta_{5/2}$ system; and the (0,0) and (1,0) bands of $[13.9]\,^2\Pi_{3/2}$-$A\,^2\Pi_{3/2}$ system. Spectra of isotopic molecules confirmed the vibrational quantum number assignment of the observed bands. Least-squares fit of rotationally resolved transition lines yielded accurate molecular constants for the $v=0-2$ levels of the $[13.3]\,^2\Sigma^+$ state, the $v=0$ level of the $A\,^2\Pi_{3/2}$, and the $v=1$ level of the $X\,^2\Delta_{5/2}$ state. The vibrational separation, $\Delta G_{1/2}$, of the ground state was measured to be 276.674 cm^{-1}. With the observation of the $[13.9]\,^2\Pi_{3/2}$-$A\,^2\Pi_{3/2}$ and $[13.9]\,^2\Pi_{3/2}$-$X\,^2\Delta_{5/2}$ transitions, we accurately determined the energy separation between the $A\,^2\Pi_{3/2}$ and the $X\,^2\Delta_{5/2}$ to be 163.847 cm^{-1}. This confirms that the order of the $A\,^2\Pi_{3/2}$ and $X\,^2\Delta_{5/2}$ states in NiI is reversed when compared with other nickel monohalides. © *2004 American Institute of Physics.*
[DOI: 10.1063/1.1806417]

I. INTRODUCTION

Recent interests in transition-metal monohalides are both in basic research[1–3] and practical applications.[4,5] Transition-metal monohalides can be considered as simple model systems that provide knowledge of chemical bonding involving electrons in the *d* orbitals. In the first transition-metal period, the nickel monohalides received much attention lately. Amongst these nickel monohalides, good knowledge of the electronic structure of the ground and some low-lying electronic states for NiF (Refs. 6–17), NiCl (Refs. 18–24), and NiBr (Refs. 25–31) has been obtained. These three isovalent molecules all have the same $X\,^2\Pi_{3/2}$ as their ground state, and the $A\,^2\Delta_{5/2}$ state is lying higher in energy. Tam *et al.*[32] recently studied the visible spectrum of NiI using laser-induced fluorescence (LIF) spectroscopy and found that the ground state is the $X\,^2\Delta_{5/2}$ state, which is different from the other isovalent nickel monohalides. However, they did not observe any electronic transition relating to the low-lying $A\,^2\Pi_{3/2}$ state. It is essential to obtain evidence and also locate the low-lying $A\,^2\Pi_{3/2}$ state to confirm beyond doubt that the ground state of NiI is $X\,^2\Delta_{5/2}$ state.

In this paper, we describe the analysis of seven electronic transition bands, belonging to three electronic systems, recorded using the technique of laser vaporization/reaction free-jet expansion and LIF spectroscopy. The seven molecular transition bands are all crowded in the near infrared region and spread over a range of only about 900 cm^{-1}. The three electronic transitions identified are the $[13.3]\,^2\Sigma^+$-$A\,^2\Pi_{3/2}$, $[13.9]\,^2\Pi_{3/2}$-$X\,^2\Delta_{5/2}$, and $[13.9]\,^2\Pi_{3/2}$-$A\,^2\Pi_{3/2}$ systems. The measured line positions for both isotopic molecules, ^{58}NiI and ^{60}NiI, were fit to energy-level expressions to retrieve accurate vibrational and rotational constants for the $[13.9]\,^2\Pi_{3/2}$, $[13.3]\,^2\Sigma^+$, $A\,^2\Pi_{3/2}$, and $X\,^2\Delta_{5/2}$ states. A comparison of available spectroscopic information of the nickel monohalides indicates that more work is required to fully characterize even the low-lying electronic states.

II. EXPERIMENT

The experimental apparatus and detailed procedure for producing transition-metal containing molecules using laser vaporization/reaction free-jet expansion and LIF spectroscopy have been described in earlier publications.[32,33] Only a brief description of the relevant experimental conditions for obtaining the NiI spectrum is given here. Frequency-doubled Nd:YAG laser pulses with 5–6 mJ were focused onto the surface of a nickel rod to generate nickel atoms. A pulsed valve, with appropriate delay, released a gas mixture of about 2% CH_3I seeded in argon to react with the nickel atoms for producing NiI. Jet-cooled NiI molecules were excited by a continuous-wave (cw) ring Ti:sapphire laser equipped with short wavelength optics in the near infrared region and pumped by an argon-ion laser. The LIF signal was collected by a lens system and detected by a photomultiplier tube. A linewidth of about 250 MHz was obtained. The wavelength of the Ti:sapphire laser was measured using a wavemeter with an accuracy about one part in 10^7. The absolute accuracy of the measured line position is below ± 0.002 cm^{-1}. The electronic transition spectrum of NiI was obtained by connecting hundreds of scans using the wavemeter reading.

III. RESULTS AND DISCUSSION

A. Low-resolution broadband spectrum

Low-resolution LIF spectrum of NiI in the near infrared region between 13 000 and 14 000 cm^{-1} has been recorded.

[a]Present address: Department of Chemistry, University of Alberta, Edmonton, Alberta, Canada.
[b]Author to whom correspondence should be addressed. Fax: (852) 2857-1586. Electronic mail: hrsccsc@hku.hk

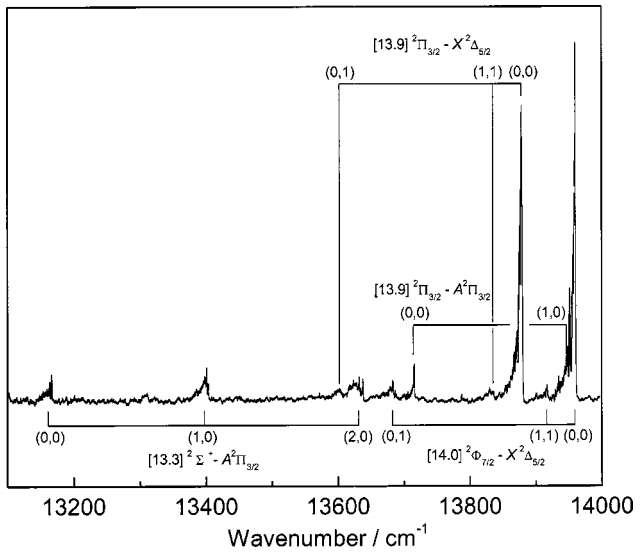

FIG. 1. Low-resolution LIF spectrum of the $[13.3]\,^2\Sigma^+$-$A\,^2\Pi_{3/2}$, $[13.9]\,^2\Pi_{3/2}$-$A\,^2\Pi_{3/2}$, and $[13.9]\,^2\Pi_{3/2}$-$X\,^2\Delta_{5/2}$ band systems of the NiI.

Figure 1 depicts a broadband low-resolution scan of the NiI spectrum. The two strong bands at 13 878 and 13 959 cm^{-1} are the (0,0) band of the $[13.9]\,^2\Pi_{3/2}$-$X\,^2\Delta_{5/2}$ transition and the (0,0) band of the $[14.0]\,^2\Phi_{7/2}$-$X\,^2\Delta_{5/2}$ transition, respectively. Since the $[14.0]\,^2\Phi_{7/2}$-$X\,^2\Delta_{5/2}$ transition shows hyperfine structure,[34,35] we have work in progress to further resolve the hyperfine components. The result of the study will be reported elsewhere. Detailed analysis of the (0,0) band of the $[13.9]\,^2\Pi_{3/2}$-$X\,^2\Delta_{5/2}$ transition with line positions and molecular constants were reported in our earlier publication.[32] The weaker bands in Fig. 1 are either hot bands or transition bands involving low-lying excited states. The jet-cooled molecular source is known to produce molecules at relatively low temperature, which favors the population of molecules in the $v=0$ level of the ground state. The population of higher vibrational levels of the ground state or any excited states would be very much reduced, and the transition intensity is expected to be much weaker. Using our apparatus, even the weak bands are of sufficient intensity to be recorded under high resolution. Seven bands belonging to three electronic transition systems, were identified and assigned: the (0,0), (1,0), and (2,0) bands of $[13.3]\,^2\Sigma^+$-$A\,^2\Pi_{3/2}$ transition; the (1,1) and (0,1) bands of $[13.9]\,^2\Pi_{3/2}$-$X\,^2\Delta_{5/2}$ transition; and the (0,0) and (1,0) bands of $[13.9]\,^2\Pi_{3/2}$-$A\,^2\Pi_{3/2}$ transition. Amongst these transition systems, the $[13.9]\,^2\Pi_{3/2}$-$X\,^2\Delta_{5/2}$ transition had been discussed in our earlier paper,[32] however, in the present work, the (0,1) and the (1,1) hot bands were recorded. Figure 2 shows all the electronic transitions observed so far for NiI.

B. $[13.3]\,^2\Sigma^+$-$A\,^2\Pi_{3/2}$ system

This transition system is slightly more complex than the other observed NiI system, this is because a transition between a $^2\Sigma^+$ state in case (b) and a $^2\Pi$ state in case (a) coupling scheme results in three main and three satellite branches, namely, P_2, Q_2, R_2, P_{12}, Q_{12}, and R_{12}. Figure 3 shows a portion of the (2,0) band of this transition. The P_2, Q_2, and R_2 branches form heads at 13 631.8, 13 633.5, and 13 636.7 cm^{-1}, respectively, and the P_{12}, Q_{12}, and R_{12} branches lie in the lower-energy region. The (0,0), (1,0), and (2,0) bands of ^{58}NiI and ^{60}NiI were recorded and analyzed. The observed line positions were fit to the following expressions:

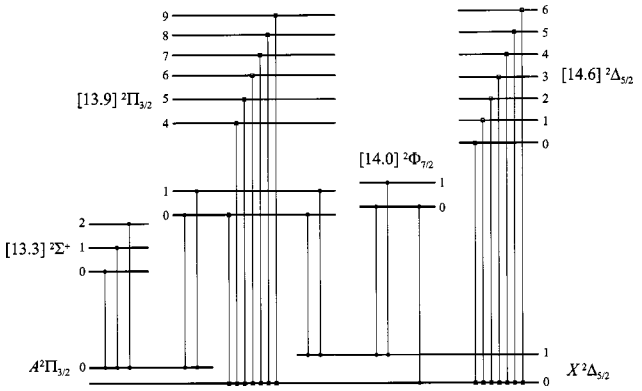

FIG. 2. Observed electronic transitions of NiI.

The upper-state $^2\Sigma^+$ term values:

$$F_1'(J)=v_o+B'(J'-\tfrac{1}{2})(J'+\tfrac{1}{2}) - D'[(J'-\tfrac{1}{2})(J'+\tfrac{1}{2})]^2+\tfrac{1}{2}\gamma(J'-\tfrac{1}{2}), \quad (1)$$

$$F_2'(J)=v_o+B'(J'+\tfrac{1}{2})(J'+3/2) - D'[(J'+\tfrac{1}{2})(J'+3/2)]^2-\tfrac{1}{2}\gamma(J'+3/2), \quad (2)$$

The lower-state $^2\Pi_{3/2}$ term values:

$$F_2''(J)=B''J''(J''+1)-D''[J''(J''+1)]^2, \quad (3)$$

where the usual meaning of $'$ and $''$ are, respectively, for the upper and lower states, v_o is the band origin of the upper state, B and D are the rotational constants and its centrifugal distortion constants, and γ is the spin-rotation constant.

Since no Λ-type doubling has been observed, the corresponding Λ-type doubling parameter was not included in the

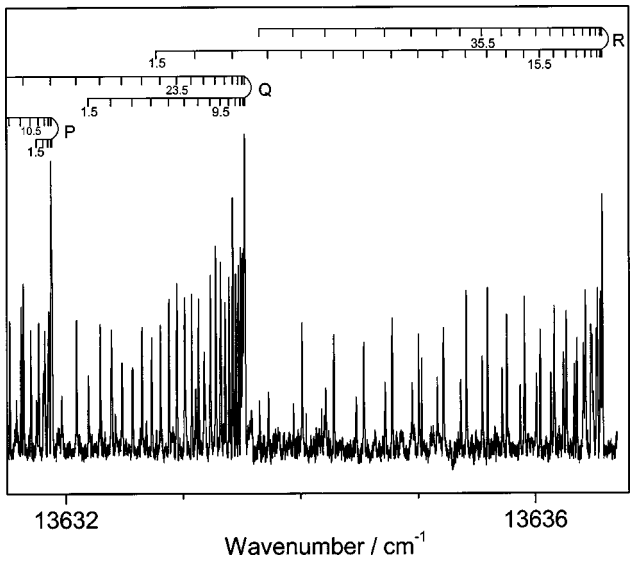

FIG. 3. (2,0) band of the $[13.3]\,^2\Sigma^+$-$A\,^2\Pi_{3/2}$ transition of ^{58}NiI.

TABLE I. Molecular constants for the $[13.9]\,^2\Pi_{3/2}$, $[13.3]\,^2\Sigma^+$, $A\,^2\Pi_{3/2}$, and $X\,^2\Delta_{5/2}$ states of NiI (cm^{-1}).

State	Parameter	^{58}NiI	^{60}NiI
$[13.9]\,^2\Pi_{3/2}$	T_1	14 112.0620(5)	14 109.5929(6)
	B	0.068 407(3)	0.066 875(3)
	10^8D	0.57(25)	1.3(3)
	T_0	13 878.6411(3)	13 878.8373(3)
	B	0.068 688(2)	0.067 149(2)
	10^8D	0.47(18)	1.4(3)
$[13.3]\,^2\Sigma^+$	T_2	13 795.4281(2)	13 790.2511(2)
	B	0.069 2701(5)	0.067 724(1)
	10^8D	1.08(3)	1.61(9)
	γ	−0.323 82(1)	−0.316 44(2)
	T_1	13 561.1309(2)	13 558.6152(3)
	B	0.069 5551(5)	0.067 997(1)
	10^8D	0.85(2)	1.2(1)
	γ	−0.325 80(1)	−0.318 29(1)
	T_0	13 325.3636(2)	13 325.5413(2)
	B	0.069 8401(6)	0.068 2747(6)
	10^8D	1.02(2)	1.64(2)
	γ	−0.327 82(2)	−0.320 27(1)
$A\,^2\Pi_{3/2}$	T_0	163.8471(4)	163.8761(5)
	B	0.076 847(2)	0.075 117(3)
	10^8D	0.9(2)	1.5(3)
$X\,^2\Delta_{5/2}$	T_1	276.6744(6)	
	B	0.076 552(2)	
	10^8D	0.38(8)	

Hamiltonian. Transition line positions were calculated by taking the difference between the upper- and lower-state term values. Similar to other transition systems analyzed, initially, individual band-by-band least-squares fit was performed to each observed band, and eventually, all measured line positions were merged in a grand least-squares fit. Molecular constants obtained are listed in Table I.

C. $[13.9]\,^2\Pi_{3/2}$-$A\,^2\Pi_{3/2}$ system

The (0,0) and (1,0) bands observed have band heads at 13 715.4 and 13 948.8 cm^{-1}, respectively. The strong P and R branches are consistent with a $\Delta\Lambda=0$ transition. The clear assignment of the first lines of the P, Q, and the R branches established the observed transition as $[13.9]\,^2\Pi_{3/2}$-$A\,^2\Pi_{3/2}$ transition. Figure 4 shows the band head region of the (0,0) band. The measured line positions were again fit using the following expression:

$$\upsilon=\upsilon_o+\{B'J'(J'+1)-D'[J'(J'+1)]^2\}-\{B''J''(J''+1)-D''[J''(J''+1)]^2\}. \quad (4)$$

Initially, a band-by-band least-squares fit was performed to line positions. Subsequently, after we realized that the upper state is in common with the $[13.9]\,^2\Pi_{3/2}$-$X\,^2\Delta_{5/2}$ transition, the line positions were merged together in the final grand least-squares fit.

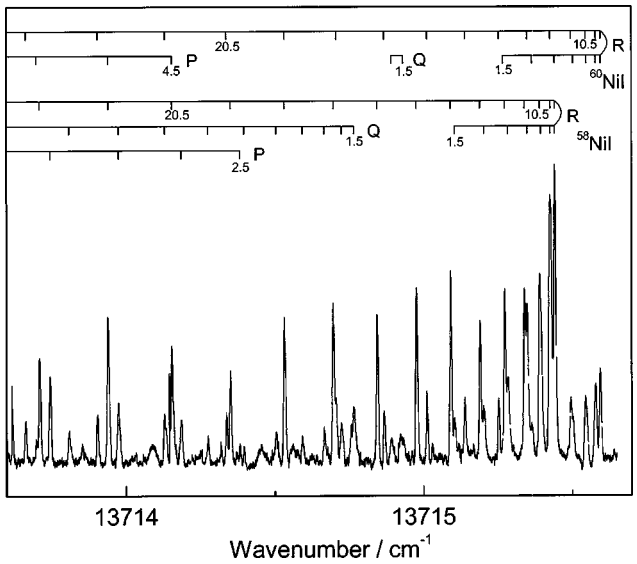

FIG. 4. (0,0) band of the $[13.9]\,^2\Pi_{3/2}$-$A\,^2\Pi_{3/2}$ transition of NiI.

D. $[13.9]\,^2\Pi_{3/2}$-$X\,^2\Delta_{5/2}$ system

The weaker transition bands with heads occurring at 13 603 and 13 836 cm^{-1} are readily assigned as the (0,1) and the (1,1) hot bands of the $[13.9]\,^2\Pi_{3/2}$-$X\,^2\Delta_{5/2}$ transition. The first lines of the P, Q, and R branches are with $J=2.5$, which indicates the $\Omega''=2.5$ and $\Omega'=1.5$ of the lower and upper electronic states, respectively. The P and Q branches are stronger than the R branch, which agrees well with the $\Delta\Lambda=-1$ transition. Since the upper state of this system is the same as the $[13.9]\,^2\Pi_{3/2}$-$A\,^2\Pi_{3/2}$ transition, a merged least-squares fit gave an accurate determination of the energy separation between the $A\,^2\Pi_{3/2}$ state and the $X\,^2\Delta_{5/2}$ state. Due to the fact that only relatively low J lines were measured in this work, in the merged fit, the rotational constant of the $X\,^2\Delta_{5/2}$ state was set to a value published by Tam *et al.*,[32] and the centrifugal distortion constant for the $X\,^2\Delta_{5/2}$ state was derived from the Kratzer relation. The results are listed in Table I.

A list of the measured line positions of the observed transition bands of the $[13.3]\,^2\Sigma^+$-$A\,^2\Pi_{3/2}$, $[13.9]\,^2\Pi_{3/2}$-$X\,^2\Delta_{5/2}$, and $[13.9]\,^2\Pi_{3/2}$-$A\,^2\Pi_{3/2}$ systems of the ^{58}NiI and ^{60}NiI isotopic molecules is available from the EPAPS.[36] The root-mean-squares error of the merged grand least-squares fit was 0.0016 cm^{-1}.

E. Isotopic relationship between ^{58}NiI and ^{60}NiI

Our vibrational quantum number assignment of the upper states was confirmed by examining the isotopic relationship of the observed bands. Molecular parameters of isotopic molecules are approximately related by different powers of the mass dependence $\rho=(\mu/\mu_i)^{1/2}$, which μ and μ_i are, respectively, the reduced mass of ^{58}NiI and ^{60}NiI. Table II compares the observed and calculated equilibrium molecular constants. The agreement between the calculated and observed isotopic constants is excellent.

TABLE II. Equilibrium molecular constants for the $[13.3]\,^2\Sigma^+$ state of ^{58}NiI and ^{60}NiI (cm^{-1}).

State	Parameter	^{58}NiI	^{60}NiI[a] Observed	^{60}NiI[a] Calculated[b]
$[13.3]\,^2\Sigma^+$	T_e	13 206.929	13 208.467	—
	ω_e	237.237	234.508	234.509
	$\omega_e x_e$	0.735	0.718	0.718
	B_e	0.069 980	0.068 142	0.068 380
	α_e	0.000 285	0.000 275	0.000 278

[a]Uncertainty for the parameter could not be obtained from the least-square fit.
[b]Molecular constants were calculated using isotopic relationships and the values from ^{58}NiI.

F. Discussion

The molecular-orbital (MO) energy-level diagram and the low-lying electronic states of NiI have been discussed earlier.[32] The known electronic states of nickel monohalides are expected to arise from the electronic configurations as follows:

$$(2\sigma)^2(2\pi)^4(1\delta)^3 \quad X\,^2\Delta_i, \tag{5}$$

$$(2\sigma)^2(2\pi)^3(1\delta)^4 \quad A\,^2\Pi_i, \tag{6}$$

$$(2\sigma)^1(2\pi)^4(1\delta)^4 \quad B\,^2\Sigma^+, \tag{7}$$

$$(2\sigma)^1(2\pi)^4(1\delta)^3(3\sigma)^1 \quad (2)\,^2\Delta_i, {}^4\Delta_i, \tag{8}$$

$$(2\sigma)^2(2\pi)^3(1\delta)^3(3\sigma)^1 \quad (2)\,^2\Pi_i, {}^4\Pi_i; (2)\,^2\Phi_i, {}^4\Phi_i, \tag{9}$$

$$(2\sigma)^2(2\pi)^2(1\delta)^4(3\sigma)^1 \quad {}^2\Sigma^+, {}^2\Sigma^-, {}^2\Delta, {}^4\Sigma^-. \tag{10}$$

The $[13.3]\,^2\Sigma^+$-$A\,^2\Pi_{3/2}$ transition observed, in the present work, is likely to arise from the promotion of an electron from the 2π MO to the 3σ MO. Similarly, the $[13.9]\,^2\Pi_{3/2}$-$A\,^2\Pi_{3/2}$ transition arises from the promotion of an electron from the 1δ MO to the 3σ MO. The electronic states of NiI and the isovalent molecules NiF, NiCl, and NiBr are quite similar. From the molecular constants obtained in Tables I and II, the equilibrium bond length, r_e, of the $[13.3]\,^2\Sigma^+$ state was measured to be 2.4608 Å and the effective bond length, r_o, of the $A\,^2\Pi_{3/2}$ and the $X\,^2\Delta_{5/2}$ states were determined to be 2.3484 and 2.3479 Å, respectively. Since the $[13.3]\,^2\Sigma^+$ state arises from the occupation of the antibonding 3σ MO, it is consistent that the bond length of the $[13.3]\,^2\Sigma^+$ state is longer than the ground $X\,^2\Delta_{5/2}$ state. However, the 2π and the 1δ MO are, respectively, bonding and nonbonding orbitals; it is reasonable that the bond length of the $A\,^2\Pi_{3/2}$ and $X\,^2\Delta_{5/2}$ states are similar. With the observation of the $[13.9]\,^2\Pi_{3/2}$-$A\,^2\Pi_{3/2}$ and $[13.9]\,^2\Pi_{3/2}$-$X\,^2\Delta_{5/2}$ transitions, we accurately determined that the $A\,^2\Pi_{3/2}$ state is 163.847 cm^{-1} above the $X\,^2\Delta_{5/2}$ state. The energy order of the $^2\Pi_{3/2}$ and the $^2\Delta_{5/2}$ states in NiI is confirmed to be different from the isovalent NiF, NiCl, and NiBr molecules. Furthermore, the vibrational separation, $\Delta G_{1/2}$, of the $X\,^2\Delta_{5/2}$ state is measured to be 276.67 cm^{-1}.

Table III lists the known molecular spectroscopic constants for the ground and the low-lying electronic states of the nickel monohalides. Even though only partial knowledge of the electronic states is available, a comparison of these states shows some general observations that are helpful for locating the unobserved states. First, a low-lying $^2\Phi_{7/2}$ state has been observed for NiF and NiI but not for NiCl and NiBr, and the observed bands belong to a $^2\Phi_{7/2}$-$A\,^2\Delta_{5/2}$ transition. From the comparison of different nickel monohalides, the low-lying $^2\Phi_{7/2}$ state is likely to arise from the electronic configuration (9). We would expect that the $^2\Phi_{7/2}$-$A\,^2\Delta_{5/2}$ transition of NiCl and NiBr also lie in the near infrared region. Since NiCl and NiBr have the $X\,^2\Pi_{3/2}$ ground state, which is orbitally forbidden to reach the $^2\Phi_{7/2}$ state, however, the $A\,^2\Delta_{5/2}$ is only 157 and 37 cm^{-1}, respectively, above the ground state. It is reasonable to expect that the $A\,^2\Delta_{5/2}$ state can be appreciably populated by a relatively "warm" free-jet, and the $^2\Phi_{7/2}$-$A\,^2\Delta_{5/2}$ transition could be observed using either absorption or LIF spectroscopy. Second, the observed spin–orbit separation of the $A\,^2\Delta$ state is 1394 and 1488 cm^{-1} of NiF and NiCl, respectively, and the Ni atom dominates the spin-orbit interaction of the nickel monohaildes.[32] We would expect the $A\,^2\Delta_{3/2}$ state of the NiBr and the $X\,^2\Delta_{3/2}$ state of NiI are about 1400 cm^{-1} above their corresponding $A\,^2\Delta_{5/2}$ and $X\,^2\Delta_{5/2}$ states. However, unlike the $A\,^2\Delta_{5/2}$ state, it is very difficult to populate the high-lying $A\,^2\Delta_{3/2}$ component with an appreciable number density, and the best way to observe any transition to the $A\,^2\Delta_{3/2}$ state is through emission spectroscopy. Finally, it is interesting to note that the $^2\Sigma^+$ state is commonly observed in all the nickel monohalides. The $B\,^2\Sigma^+$ state of NiF and NiCl arise from the electronic configuration (7) and lie about 1574 and 1768 cm^{-1} above the ground state. In view of the similar nature in chemical bonding and electronic configurations between the nickel monohalides, the $B\,^2\Sigma^+$ state of the NiBr and NiI are also expected to be low lying in energy. Similar to the $^2\Delta_{3/2}$ component of the $A\,^2\Delta_i$ state of NiBr and the $X\,^2\Delta_i$ state of NiI, the $B\,^2\Sigma^+$ state of NiBr and NiI would be difficult to be populated and is appropriate to be studied using emission spectroscopy. The $[12.3]\,^2\Sigma^+$ state of NiCl, $[12.6]\,^2\Sigma^+$ state of NiBr, and the $[13.3]\,^2\Sigma^+$ state of NiI are expected to arise from the electronic configuration (10), therefore, the corresponding $^2\Sigma^+$ state of NiF is expected to lie in comparable energy. Chen and co-workers,[12–14] using LIF spectroscopy, and Bernath and co-workers,[17,20] using Fourier transform (FT) spectroscopy, recently studied many electronic transitions in the visible region above 600 nm and also in the near infrared region[17] from 9500 to 13 000 cm^{-1}, but nothing was reported for a gap between 13 000 and 16 000 cm^{-1}. It is worthwhile to examine this spectral region using either LIF or FT emission spectroscopy to study the expected $^2\Sigma^+$ state of NiF. The $[0.25]\,^2\Sigma^+$ state of NiF was first observed by Dufour and Princhemel[10] using the FT spectroscopy and confirmed by microwave experiments,[15] however, it is not possible to account for the existence of such a low-energy $^2\Sigma^+$ state using electronic configurations derived from the molecular-orbital level diagram, and the spin-rotation constant of this state is also unrealistically large. We agree with the suggestion of Bernath and co-workers[19] that the $[0.25]\,^2\Sigma^+$ state should be reassigned as the $\Omega=\frac{1}{2}$ component of the $X\,^2\Pi$ state. The large spin-rotation splitting observed could be ascribed to as the Λ-type

TABLE III. Spectroscopic constants for the low-lying electronic states of nickel monohalides (cm^{-1}).

NiF		NiCl		NiBr		NiI	
$X\ ^2\Pi_{3/2}$	$B_o=0.387\ 81$ (Ref. 17) r_o (Å)=1.7403	$X\ ^2\Pi_{3/2}$	$B_o=0.181\ 50$ (Ref. 18) r_o (Å)=2.0637 $\omega_e=425.63$	$X\ ^2\Pi_{3/2}$	$B_o=0.104\ 60$ (Ref. 30) r_o (Å)=2.1963	$X\ ^2\Delta_{5/2}$	$B_o=0.076\ 86$ (Ref. 32) r_o (Å)=2.3479 $\Delta G_{1/2}=276.674$
$[0.25]\ ^2\Sigma^+$ or $X\ ^2\Pi_{1/2}$	$T_o=251.25$ (Ref. 15) $B_o=0.390\ 01$ r_o (Å)=1.7381 $\gamma=-0.960$	$A\ ^2\Delta_{5/2}$	$T_e=157.70$ (Ref. 18) $B_e=0.184\ 31$ r_e (Å)=2.0480 $\omega_e=435.52$	$A\ ^2\Delta_{5/2}$	$T_o=37.46$ (Ref. 30) $B_o=0.107\ 71$ r_o (Å)=2.1644	$A\ ^2\Pi_{3/2}$	$T_o=163.847$ $B_o=0.076\ 85$ r_o (Å)=2.3484
$A\ ^2\Delta_{5/2}$	$T_o=829.48$ (Ref. 17) $B_o=0.388\ 54$ r_o (Å)=1.7386 $\omega_e=646.10$	$X\ ^2\Pi_{1/2}$	$T_e=385.666$ (Ref. 20) $B_e=0.180\ 78$ r_o (Å)=2.0678	$[12.6]\ ^2\Sigma^+$	$T_e=12\ 412.323$ (Ref. 30) $B_e=0.098\ 61$ r_o (Å)=2.2620 $\gamma=-0.4464$	$[13.3]\ ^2\Sigma^+$	$T_e=13\ 206.929$ $B_e=0.069\ 98$ r_e (Å)=2.4608 $\omega_e=237.237$ $\gamma=-0.325$
$B\ ^2\Sigma^+$	$T_o=1574.106$ (Ref. 16) $B_o=0.386\ 00$ r_o (Å)=1.7471 $\gamma=-0.1495$	$A\ ^2\Delta_{3/2}$	$T_o=1645.83$ (Ref. 20) $B_o=0.182\ 29$ r_o (Å)=2.0593	$[13.2]\ ^2\Pi_{3/2}$	$T_e=13\ 047.81$ (Ref. 30) $B_e=0.096\ 94$ r_e (Å)=2.2814 $\omega_e=292.97$	$[13.9]\ ^2\Pi_{3/2}$	$T_e=13\ 761.28$ (Ref. 32) $B_e=0.068\ 40$ r_e (Å)=2.4834 $\omega_e=235.09$
$A\ ^2\Delta_{3/2}$	$T_e=2223.56$ (Ref. 16) $B_o=0.388\ 35$ r_o (Å)=1.7390	$B\ ^2\Sigma^+$	$T_o=1768.07$ (Ref. 19) $B_o=0.179\ 85$ r_o (Å)=2.0732 $\gamma=-0.1154$			$[14.0]\ ^2\Phi_{7/2}$	$T_o=13\ 958.87$ (Ref. 34) $B_o=0.069\ 58$ r_o (Å)=2.4680 $\Delta G_{1/2}=233.911$
$[11.1]\ ^2\Pi_{3/2}$	$T_o=11\ 096.05$ (Ref. 17) $B_o=0.367\ 11$ r_o (Å)=1.7886	$[9.1]\ ^2\Pi_{3/2}$	$T_o=9101.261$ (Ref. 24) $B_o=0.171\ 773$ r_o (Å)=2.1214			$[14.6]\ ^2\Delta_{5/2}$	$T_e=14\ 468.67$ (Ref. 32) $B_e=0.067\ 50$ r_e (Å)=2.5081 $\omega_e=230.56$
$[12.0]\ ^2\Phi_{7/2}$	$T_o=12\ 008.924$ (Ref. 17) $B_o=0.365\ 92$ r_o (Å)=2.7944 $\Delta G_{1/2}=620.915$	$[12.3]\ ^2\Sigma^+$	$T_o=12\ 252.19$ (Ref. 25) $B_o=0.179\ 94$ r_o (Å)=2.0726 $\gamma=-0.1136$				
		$[13.0]\ ^2\Pi_{3/2}$	$T_o=12\ 959.25$ (Ref. 13) $B_o=0.167\ 69$ r_o (Å)=2.1470				

doubling of the $^2\Pi_{1/2}$ state. Table III also shows that the spin-rotation constants for the $^2\Sigma^+$ states of all the nickel monohalides are negative. Since the spin-rotation constant is composed of both the first- and second-order contributions from, respectively, the magnetic dipole-dipole interaction, and the cross terms between the L-uncoupling and spin–orbit operators. Both the contributions connect the $^2\Sigma$ state to various $^2\Pi$ electronic states. The observed γ value is the resultant of all the contributions. Simard *et al.*[37] discussed the different interactions between $^2\Sigma$ and $^2\Pi$ electronic states giving rise to various size and sign of the γ value for the $^2\Sigma^+$ state. They concluded that the negative sign observed in the ground and low-lying $^2\Sigma^+$ states of the many isovalent molecules including YO molecule is arisen mainly from the interaction between the $^2\Sigma^+$ state and a $^2\Pi$ state with the electronic configuration similar to (6). We noticed that all the observed $^2\Sigma^+$ states of the nickel monohalides have relatively large and negative spin-rotation constant. Since the electronic configurations of nickel monohalides and those discussed by Simard *et al.*[37] are quite similar, and the low-lying $A\ ^2\Pi$ state also arises from electronic configuration (6), we would expect that the $A\ ^2\Pi$ state in the nickel monohalides is also responsible for giving rise to the negative γ values for the $^2\Sigma^+$ states in the nickel monohalides.

ACKNOWLEDGMENTS

The work described here was supported by a grant from the Committee on Research and Conference Grants. The authors thank Mr. P. M. Yeung and Dr. J. W.-H. Leung for providing technical help.

[1] S. R. Langhaff and C. W. Bauschliher, Jr., Annu. Rev. Phys. Chem. **39**, 181 (1988).
[2] E. Hirota, Annu. Rep. Prog. Chem., Sect. C: Phys. Chem. **96**, 95 (2000).
[3] P. F. Bernath, Annu. Rep. Prog. Chem., Sect. C: Phys. Chem. **96**, 177 (2000).
[4] C. N. Rao, Annu. Rev. Phys. Chem. **40**, 291 (1989).
[5] M. Wojuechowsba, J. Habu, S. Lomnicki, and J. Stoh, J. Mol. Catal. A: Chem. **141**, 155 (1999).
[6] C. Dufour, P. Carette, and B. Pinchemel, J. Mol. Spectrosc. **148**, 303 (1991).
[7] C. Dufour, I. Hikmet, and B. Pinchemel, J. Mol. Spectrosc. **158**, 392 (1993).
[8] C. Dufour, I. Hikmet, and B. Pinchemel, J. Mol. Spectrosc. **165**, 477 (1994).
[9] A. Bouddou, C. Dufour, and B. Pinchemel, J. Mol. Spectrosc. **168**, 477 (1994).
[10] C. Dufour and B. Princhemel, J. Mol. Spectrosc. **173**, 70 (1995).
[11] C. Focsa, C. Dufour, and B. Pinchemel, J. Mol. Spectrosc. **182**, 65 (1997).
[12] Y. Chen, J. Jin, C. Hu, X. Yang, X. Ma, and C. Chen, J. Mol. Spectrosc. **203**, 37 (2000).
[13] J. Jin, Y. Chen, X. Yang, Q. Ran, and C. Chen, J. Mol. Spectrosc. **208**, 18 (2001).

[14] J. Jin, Q. Ran, X. Yang, Y. Chen, and C. Chen, J. Phys. Chem. A **105**, 11177 (2001).
[15] M. Tanimoto, T. Sakamaki, and T. Okabayashi, J. Mol. Spectrosc. **207**, 66 (2001).
[16] Y. Krouti, T. Hirao, C. Dufour, A. Boulezhar, B. Pinchemel, and P. F. Bernath, J. Mol. Spectrosc. **214**, 152 (2002).
[17] B. Pinchemel, T. Hirao, and P. F. Bernath, J. Mol. Spectrosc. **215**, 262 (2002).
[18] T. Hirao, C. Dufour, B. Pinchemel, and P. F. Bernath, J. Mol. Spectrosc. **202**, 53 (2000).
[19] A. Poclet, Y. Krouti, T. Hirao, B. Pinchemel, and P. F. Bernath, J. Mol. Spectrosc. **204**, 125 (2000).
[20] Y. Krouti, A. Poclet, T. Hirao, B. Pinchemel, and P. F. Bernath, J. Mol. Spectrosc. **210**, 41 (2001).
[21] E. Yamazaki, T. Okabayashi, and M. Tanimoto, Astrophys. J. Lett. **551**, L199 (2001).
[22] L. C. O'Brien, K. M. Homann, T. L. Kellerman, and J. J. O'Brien, J. Mol. Spectrosc. **211**, 93 (2001).
[23] J. J. O'Brien, J. S. Miller, and L. C. O'Brien, J. Mol. Spectrosc. **211**, 93 (2002).
[24] S. Tumturk, L. C. O'Brien, and J. J. O'Brien, J. Mol. Spectrosc. **225**, 225 (2004).
[25] C. A. Rice and L. C. O'Brien, J. Mol. Spectrosc. **221**, 131 (2003).
[26] A. B. Darji and N. R. Shah, Curr. Sci. **48**, 349 (1979).
[27] R. Gopal and M. M. Joshi, Curr. Sci. **50**, 1061 (1981).
[28] R. Gopal and M. M. Joshi, Indian J. Phys., B **59**, 309 (1985).
[29] S. P. Reedy, N. Narayana, and P. T. Rao, Opt. Pura Apl. **20**, 69 (1987).
[30] J. W.-H. Leung, X. Wang, and A. S.-C. Cheung, J. Chem. Phys. **117**, 3694 (2002).
[31] E. Yamazaki, T. Okabayashi, and M. Tamimoto, J. Chem. Phys. **121**, 162 (2004).
[32] W. S. Tam, J. W.-H. Leung, S. Hu, and A. S.-C. Cheung, J. Chem. Phys. **119**, 12245 (2003).
[33] Q. Ran, W. S. Tam, C. Ma, and A. S.-C. Cheung, J. Mol. Spectrosc. **198**, 175 (1999).
[34] W. S. Tam, Jianjun Ye, and A. S.-C. Cheung (unpublished).
[35] A. S.-C. Cheung, Chin. J. Phys. Chem. **17**, 299 (2004).
[36] See EPAPS Document No. E-JCPSA6-121-002443 for the observed line positions of the (0,0), (1,0), and (2,0) bands of $[13.3]\ ^2\Sigma^+$-$A\ ^2\Pi_{3/2}$ transition; the (1,1) and (0,1) bands of $[13.9]\ ^2\Pi_{3/2}$-$X\ ^2\Delta_{5/2}$ transition; and the (0,0) and (1,0) bands of $[13.9]\ ^2\Pi_{3/2}$-$A\ ^2\Pi_{3/2}$ transition. A direct link to this document may be found in the online article's HTML reference section. The document may also be reached via the EPAPS homepage (http://www.aip.org/pubservs/epaps.html) or from ftp.aip.org in the directory /epaps/. See the EPAPS homepage for more information.
[37] B. Simard, J. K. G. Watson, A. J. Merer, and T. C. Steimle, J. Chem. Phys. **111**, 6148 (1999).